ISSN (Print) 1226-1750
ISSN (Online) 2233-6656
Journal of Magnetics 22(4), 649-653 (2017) https://doi.org/10.4283/JMAG.2017.22.4.649

Fabrication and Usage of a Multi-turn μ-Coil and a PR Channel Combined with a Dual-type GMR-SV Device

Jong-Gu Choi, Hoon-Mo Jung, and Sang-Suk Lee*

Department of Oriental Biomedical Engineering, Sangji University, Wonju 26339, Republic of Korea

(Received 7 October 2017, Received in final form 4 December 2017, Accepted 11 December 2017)

The dual-type GMR-SV thin films and devices with multi-turn μ-coil and PR channel for detection of red blood cell (RBC) using ion-beam deposition system and lithography process were developed and used to one biosensor. The magnetoresistance (MR) ratio of a dual-type GMR-SV device post-annealed at a temperature of 200 °C was 2.5 %, the magnetic field sensitivity (MS) was 0.6 %/Oe, and the coercivity (H_c) was 0.5 Oe. An AC magnetic field was generated in the vertical direction at the center of GMR-SV device using a multi-turn μ-coil. The magnetic beads (MB) coupled to the RBCs were controlled by the AC input current applied to a multi-turn μ-coil, measured as output signal as MR variation during a staying time of 0.5 s in the GMR-SV device. This result implies that the output signal of a dual-type GMR-SV device can analyze the detection state of the RBC passing through the center of a multi-turn μ-coil and PR channel.

Keywords : dual-type GMR-SV device, multi-turn μ-coil, PR channel, AC magnetic field, biosensor

1. Introduction

The giant magnetoresistance-spin valve (GMR-SV), which is composed of a combination of a ferromagnetic layer, a nonmagnetic layer and an antiferromagnetic layer, is sensitive to low magnetic fields [1]. GMR-SV sensor with highly sensitive magnetic properties that apply to bio-molecules was developed through semi-conductor lithography technology [2]. Many research groups reported the experimental results based on the measurement of magnetic properties of magnetic bead (MB)s or magnetic nano-particles [3]. Their researches indicated that bio-molecules and nano-particles could be detected which their magnetic properties analyzed exactly [1-4].

The GMR-SV sensor is widely used as a displacement and position sensor such as non-contact detection of movement of an in-cylinder piston in an automobile as well as a nano-biosensor [5]. In order to realize bio-electronic devices, it is necessary to establish molecular switching mechanism and operating concept of biomolecules and to design and fabricate devices for its artificial construction. There is a need for technology to systemize and integrate and control these chips [6]. This technology is a successful case of nano-technology in a relatively short period and can be considered to be very effective in other fields [7]. The frequency response can maintain any steady status from dc to 1 MHz but sharply attenuates at higher frequencies.

In this study, a dual-type GMR-SV biosensor for detecting of red blood cell (RBC) was prepared to fabricate a composited device pattern with a line width of several μm [8]. The dual-type GMR-SV film is optimized with Ta/NiFe/CoFe/Cu/CoFe/IrMn/CoFe/Cu/CoFe/NiFe/Ta multilayer structure. We have measured magnetoresistive output signals to detect MBs coupled to RBCs as a usage of GMR-SV device, multi turn μ-coil, and PR channel fabricated by Ar-ion milling, electrode deposition, and photolithography, respectively.

2. Experimental Methods

The dual-type GMR-SV film of Ta(5 nm)/NiFe(5 nm)/CoFe(3 nm)/Cu(2.5 nm)/CoFe(4 nm)/IrMn(8 nm)/CoFe(4 nm)/Cu(2.5 nm)/CoFe(3 nm)/NiFe(5 nm)/Ta(5 nm) multilayer was fabricated by using the ion beam deposition system [9]. To improve the magnetoresistive properties of all thin film samples, the heat treatment is performed in the vacuum chamber under a magnetic field of 1 kOe and at the annealing temperature of 200 °C for 1 hr [10].

In the manufacturing process of GMR-SV device, the

©The Korean Magnetics Society. All rights reserved.
*Corresponding author: Tel: +82-33-730-0415
Fax: +82-33-738-7610, e-mail: sslee@sangji.ac.kr

© 2017 Journal of Magnetics

electron cyclotron resonance (ECR) Ar-ion milling after the lithography process was used to etch an area of 2 × 18 μm^2 of thin film sample [11]. A Cu electrode was formed by the lift-off method. A multi-turn μ-coil and PR channel on the above part of GMR-SV device were fabricated by the ECR Ar-ion milling and the lift-off process after deposition of the insulating SiO_2 (100 nm) as a protection layer.

In vitro, several MBs were adsorbed on the surface of RBCs attached with high molecular weight proteins [12, 13]. To capture the MBs coupled to RBCs, a multi-turn coil wound five times having a width of about 3 μm was formed as a helical structure at the center of GMR-SV device. AC current was applied to generate a magnetic field in a direction perpendicular to the plane of multi-turn μ-coil. The magnetic field for the instant capture of RBCs passing through the center of GMR-SV device and PR channel was calculated by the computational simulation of finite element method and its distribution characteristics were investigated. To detect the output MR signal of the prepared GMR-SV device, we used a Hewlett Packard (3458A) digital multimeter, and then conditioned and stored using an NI DAQ system (Terminal Block 1320, Module 1121, and DAQcard 6306E). This data graphic was displayed on the monitor in real time. A metallurgical microscope (SAMWON Inc., KSM-BA3, Korea) and CCD camera (SAMSUNG AEROSPACE, SPC-400NA, Korea) were installed to observe the MBs coupled to RBC's movements.

3. Results and Discussion

Figure 1(a) shows a full size of GMR-SV devices fabricated by photolithography. Each device performed the effect of shape magnetic anisotropy in the easy axis direction of the applied magnetic field during deposition. The number of all devices in the size of 8 × 8 mm^2 is 66 with a width of 50 μm and a gap size of 250 μm between two electrodes of the same width, and common electrodes are arranged at the center. Figure 1(b) and 1(c) are photographs of the detailed GMR-SV devices included of multi-turn μ-coil and PR channel patterned by photo lithography, respectively. Figure 1(c) shows 8 number of devices in two groups, which are 4 number of GMR-SV device, multi turn μ-coil, and PR channel on the upper part and 4 number of only GMR-SV device with 2-probe electrode on the lower part.

Figure 2(a) shows the virtual locations of the GMR-SV device, the helical one turn coil with a width of a 50 nm thick Cu thin film to flow an electric current to capture multiple MBs coupled to RBCs. The center portion of the multi turn μ-coil coincides with the center of the GMR-SV element. The distribution of the magnetic field generated when AC of 0.1 mA and 20 kHz flows a one turn coil, as shown in Fig. 2(b). The magnetic field was calculated by using the electromagnetic finite element method and the OPERA 3D/SCALA SW program including Bio-Savart's law and Ampere's law [14, 15].

The magnetic field of the vertical component is actually used to capture several MBs coupled to RBCs. It does not affect the horizontal magnetic field sensed by the adjacent to GMR-SV element. Also, the horizontal leakage magnetic field generated by MBs does not change to the MR signal of GMR-SV device. When the AC current apply to the multi-turn μ-coil, the magnetic field at the position of z = 0 at the center of coil was calculated from 30.1 μT to 3,060 μT = 30.6 G in proportion to the current. The magnetic field at the position of z = 10 μm was decreased to one-sixth of that of z = 0. The MR signal of GMR-SV device was not changed by applying AC current of a magnitude of 10 mA to the coil. It was confirmed that the enough magnitude of magnetic field for the capture of

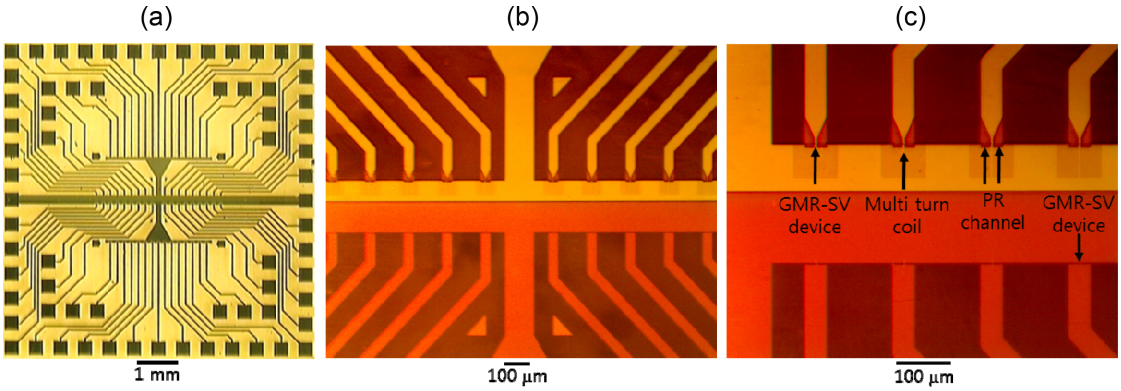

Fig. 1. (Color online) (a) Photograph of the GMR-SV devices with 2-probe electrodes of 66 number patterned by photo lithography. Photograph of the GMR-SV device, multi turn μ-coil, and PR channel (b) 10 and (c) 4 number on the upper part. Photograph of the only GMR-SV device of (b) 10 and (c) 4 number with 2-probe electrode on the lower part.

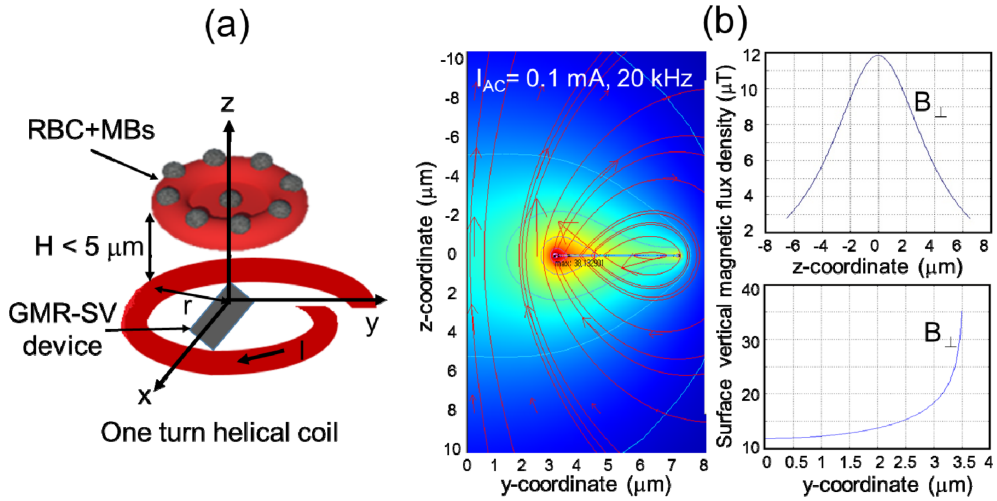

Fig. 2. (Color online) (a) Drawings for virtual locations of the GMR-SV device, the helical one turn coil, and the RBC coupled to MBs. (b) The surface vertical magnetic flux density ($B_\perp$) distributions and the calculated values of $B_\perp$ in the z- and y-coordinate of the helical one turn coil according to the applied AC current having 0.1 mA at 20 kHz. (Contour: magnetic flux density, arrow: direction, and stream line: magnetic field)

RBC is possible for the detection of MBs attached to RBC.

Figure 3(a) shows the real GMR-SV device. Figure 3(b) is a photograph in which the center portion of the coil coincides at the same position of GMR-SV device. Fig. 3(c) shows one actual shapes for a multi-turn μ-coil and GMR-SV device structure fabricated by patterning PR channel. The edge electrodes of GMR-SV devices other

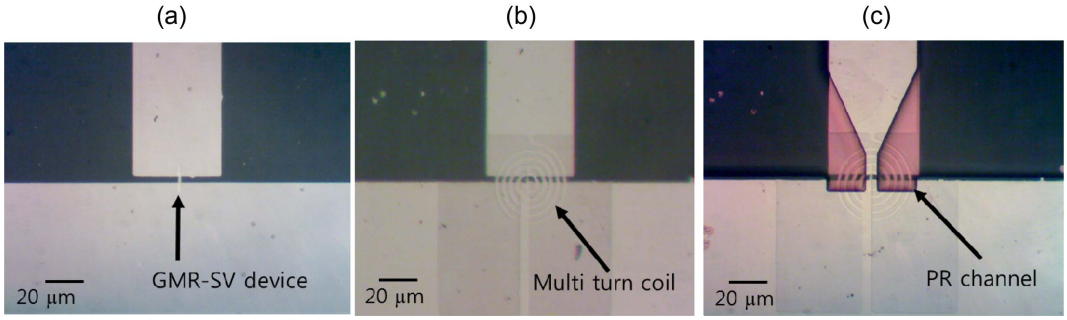

Fig. 3. (Color online) Photographs of the complex structure composed of dual-type GMR-SV μ-device, μ-coil, and PR channel; (a) dual-type GMR-SV μ-device, (b) multi-turn μ-coil, and (c) PR channel.

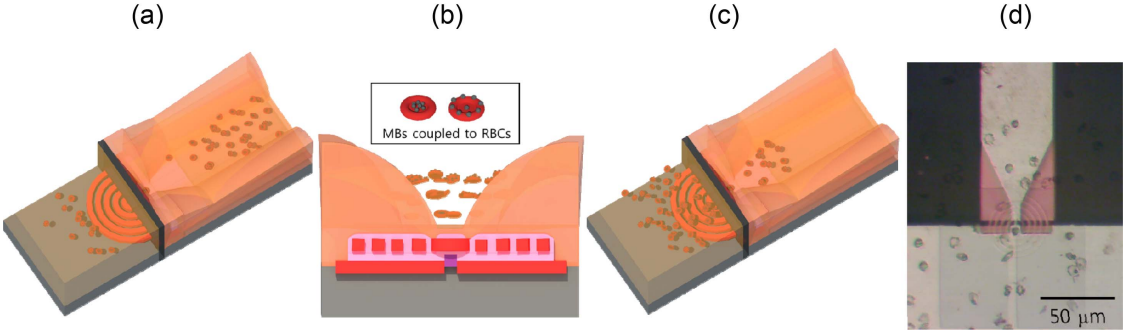

Fig. 4. (Color online) (a) One side view, (b) front view, and (c) other side view for the virtual flow with side views of two states and front cross view for MBs coupled to RBCs passed through multi-turn μ-coil with PR channel above GMR-SV device. (d) One photograph for an actual motion of RBCs combined with MBs pass to PR channel above GMR-SV device and multi-turn coil.

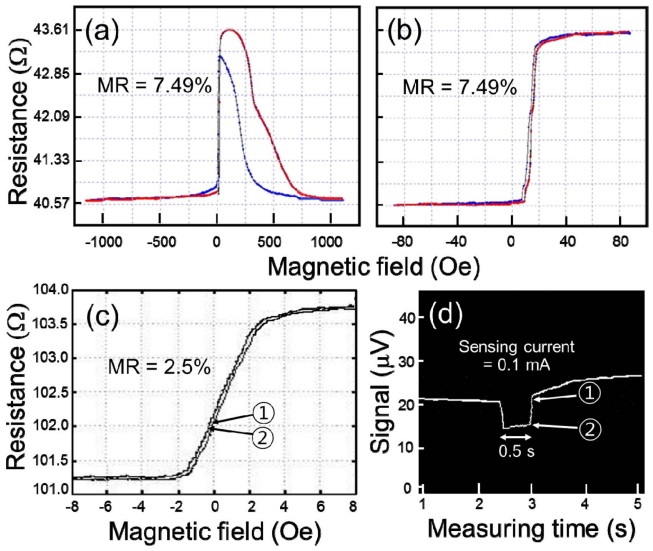

Fig. 5. (Color online) (a) Major and (b) minor MR curves of dual-type GMR-SV film. (c) Minor MR curve of GMR-SV device. (d) Output signal versus measuring time [s], when MBs coupled to RBC stayed and moved to the adjacent position around GMR-SV-device with multi-turn coil and PR channel.

than the center portion of the electrode material of all PR was coated by SiO_2 insulating layer.

The GMR-SV device with a multi-turn μ-coil and a PR channel was designed to immerse a physiological saline liquid containing RBCs combined with MBs to flow into the microtubule injector and toward the center of the complex structure with the pressure difference. The matching MBs coupled to RBCs in normal saline are to be free to move according to the flowing path of the liquid, as shown in Fig. 4(a), 4(b), and 4(c). Figure 4(a) and 4(c) shows two side views for different flowing status on the complex structure composed of μ-device of GMR-SV and multi-turn μ-coil. There are presented RBCs with MBs through to a valley in a 8 μm height and a 10 μm width of PR channel as an actual motion, as shown in Fig. 4(d).

Figure 5(a) and (b) show the major MR and the minor MR curves when changing from the dual-type GMR-SV film consisting of two pinned layers and two free layers with an antiferromagnetic IrMn thin film. We have already presented several MR curves showing typically high properties for GMR-SV thin films [16]. The MR ratio, magnetic sensitivity (MS), and coercivity (H_c) are 7.49 %, 0.8 %/Oe, and 2.0 Oe, respectively. The magnetization spin arrangement of the ferromagnetic material in the dual-type GMR-SV multilayer structure is parallel to the left and antiparallel to the right, so that the MR due to the spin-dependent scattering effect becomes the minimum and maximum value, respectively.

Figure 5(c) shows that the gentle MS of 0.6 %/Oe, the H_c of 0.5 Oe, and the MR ratio of 2.5 % are obtained from the minor MR curve of GMR-SV device measured by two probe method. When MBs coupled to RBC passing through a multi-turn μ-coil, as shown in Fig. 4, a MR of the GMR-SV element was kept at a constant value before dropping RBC with MBs. The output signal for the notation ① and ② of Fig. 5(c) corresponding to one of Fig. 5(d) means before and after passing in the center of GMR-SV device with the change of the sensing position of the minor MR curve by the abrupt variation of the sensing field in the presence of MBs coupled to RBC. An applied AC current to a multi-turn μ-coil having a frequency of 20 kHz to capture one RBC combined with MBs is 10 mA. A sensing current and a staying time at center of GMR-SV device to obtain output MR signal is 0.1 mA and 0.5 s, respectively. Output signal show the existence of one RBC during a staying time of 0.5 s, when MBs coupled to RBC stopped at the adjacent position around GMR-SV-device with a multi-turn coil and a PR channel. It suggests that several statuses of versatile membrane of RBCs combined with MBs passed through the center of μ-coil and PR channel can be analyzed by the output MR signals of GMR-SV device.

4. Conclusion

The dual-type GMR-SV film of glass/Ta/NiFe/CoFe/Cu/CoFe/IrMn/CoFe/Cu/CoFe/NiFe/Ta multuilayer structure with in-plane orthogonal easy axes controlled by the post annealing temperature of 200 ºC was prepared for applying biosensor. The dual-type GMR-SV device with multi-turn μ-coil and single PR channel was fabricated by the semiconductor lithograph process as one biosensor to detect RBCs combined with MBs. The MR properties of the dual-type GMR-SV film were a MR ratio of 7.49 %, a MS of 0.8 %/Oe, and a coercivity of 2.0 Oe. Two antiparallel states of magnetization spin arrays of the pinned and free layers in the dual-type GMR-SV multilayer films occurred the maximum MR value by the effect of spin dependence scattering.

As usage of the dual-type GMR-SV device having the MR properties of MS = 0.6 %/Oe, H_c = 0.5 Oe, and MR ratio = 2.5 %, MBs coupled to RBC can be captured by the magnetic field, which is obtained by an applying AC current of 10 mA of 20 kHz to multi-turn μ-coil. When one RBC passed on the single PR channel with a width of a 10 μm, the movement of those controlled by the electrical AC input signal applied to multi turn μ-coil. The existence of RBCs captured above the dual-type GMR-

SV device with μ-coil and PR channel confirmed as the output MR signals for detection status to analyze a new property of MBs coupled to RBC.

Acknowledgments

This work was supported by the National Research Foundation of Korea (NRF) funded by the Korea government (Ministry of Education) with the Grant No. of NRF-2016R1D1A1B03936289.

References

[1] M. D. Cubells-Beltrán, C. Reig, J. Madrenas, A. D. Marcellis, J. Santos, S. Cardoso, and P. P. Freitas, Sensors **16** 939 (2016).
[2] W. H. Lee, D. G. Hwang, and S. S. Lee, J. Magn. **14**, 18 (2009).
[3] G. Li, S. Sun, R. J. Wilson, R. L. White, N. Pourmand, and S. X. Wang, Sens. Acut. **A126**, 98 (2006).
[4] J. G. Choi, Y. S. Park, and S. S. Lee, J. Korean Magn. Soc. **22**, 173 (2012).
[5] S. X. Wang and A. M. Taratorin, Magnetic Information Storage Technology, Academic Press, New York (1999).
[6] J. W. Cho and B. H. Lee, Korean Chem. Eng. Res. **44**, 1 (2006).
[7] S. H. Hong, Physics and High Technology **18**, 16 (2009).
[8] J. Y. Lee, M. J. Kim, and S. S. Lee, New Phys. **64**, 958 (2014).
[9] J. G. Choi, S. H. Kim, S. H. Choi, and S. S. Lee, J. Korean Magn. Soc. **27**, 101 (2014).
[10] P. Khajidmaa, J. G. Choi, and S. S. Lee, J. Magn. **22**, 7 (2017).
[11] W. H. Lee, H. J. Chung, N. R. Kim, J. S. Park, S. S. Lee, and J. R. Rhee, J. Korean Magn. Soc. **25**, 162 (2015).
[12] A. I. Zhernovoy, L. M. Sharshina, and V. A. Chirukhin, Bull. Exp. Bio. Med. **3**, 844 (2001).
[13] J. S. Park, N. R. Kim, H. J. Jung, and S. S. Lee, J. Korean Magn. Soc. **25**, 16 (2015).
[14] R. D. Cook, D. S. Malkus, M. E. Plesha, and R. J. Witt, Concepts and Applications of Finite Element Analysis, John Wiley & Sons, New Jersey, 4th Ed. (2001).
[15] Cobham technical services, Opera-3d User Guide, Version 15 (2011).
[16] J. G. Choi, S. H. Kim, S. H. Choi, and S. S. Lee, J. Korean Magn. Soc. **31**, 115 (2017).